

# Lattice-gas modeling of CO adlayers on Pd(100)

Da-Jiang Liu

Ames Laboratory (USDOE), Iowa State University, Ames, Iowa 50011

(Dated: October 31, 2018)

Using a lattice-gas model with pairwise interactions, we study the ordered structures, coverage dependence of the heat of adsorption, and other experimentally observable behavior of adsorbed CO overlayers on Pd(100) single crystal surfaces. Transfer matrix and Monte Carlo methods give accurate information regarding the lattice-gas model that often contradicts simple mean-field-like analysis. We demonstrate the usefulness of the model by reproducing experimental results over a large range of pressures and temperatures.

## I. INTRODUCTION

CO adsorption on metal surfaces has been studied extensively as a benchmark system for chemisorption. In particular, great deal of information has been accumulated during the last thirty years about CO adsorption on Pd(100) surfaces using several different experimental techniques, and under a range of pressures and temperatures.<sup>1,2,3,4</sup> There are also detailed theoretical studies of CO adsorption on Pd(100) using first-principles approaches.<sup>5,6</sup> However, surprisingly, no extensive statistical mechanics studies have been performed to precisely determine adlayer ordering and phase transitions for this system. This is a significant omission since such analysis provides strong constraints on the type and magnitude of adspecies interactions. It also provides a reliable determination of thermodynamic quantities, which is not possible with simplified analyses. Such information is invaluable in interpreting other experiments, e.g., related to CO adsorption energies.

A long-standing motivation for such detailed studies of simple chemisorption systems is to provide insight into catalytic surface reactions. It is also well-recognized that ordering and islanding of reactants will limit the utility or validity of mean-field type rate equation treatments of the reaction kinetics.<sup>7</sup> Hence, accurate and robust atomistic modeling of adlayer structure for individual reactants is a crucial first step in building realistic atomistic model of related surface reactions, e.g., for CO oxidation on Pd(100).<sup>8</sup>

In this paper, we develop and analyze a lattice-gas (LG) model for CO adlayers on Pd(100). Our focus is on equilibrium aspects of this system, since molecularly adsorbed CO can diffuse quite rapidly on this surface under normal situations facilitating adlayer equilibration. However, some nonequilibrium issues are also addressed. The main techniques used to analyze behavior of the lattice-gas model are the transfer matrix method and Monte Carlo simulation. We aim to reproduce as many experimental observations as possible using a relatively simple model. We present results regarding surface ordering below 0.5 monolayers (ML) in Sec. III, the structure of dense CO adlayers in Sec. IV, the heat of adsorption in Sec. V, and the adsorption isobars in Sec. VI.

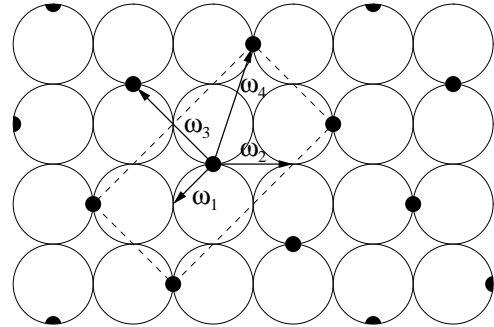


FIG. 1: Schematic of the  $c(2\sqrt{2} \times \sqrt{2})R45^\circ$  ordered structure and of the pairwise interactions used in this paper. The large open circles represent Pd atoms and the small solid circle represents CO molecules adsorbed on the bridge site of the Pd(100) surface.

## II. LATTICE-GAS MODEL FOR CO/PD(100) AND ITS ANALYSIS

Various experiments<sup>1,4,9</sup> show that adsorbed CO resides only at bridge sites on Pd(100). Thus, our modeling of equilibrated adlayer configurations allows population of bridges sites only. We note, however, that it was suggested<sup>5</sup> that during adsorption, CO is first steered towards the less favorable top sites. Thus, in more general modeling of nonequilibrium configurations under reaction conditions, it is appropriate to allow population of other sites.<sup>8</sup> Below,  $a = 2.75 \text{ \AA}$  denotes the unit cell size of Pd(100) surface.

Our LG modeling also assumes only pairwise interactions between CO adsorbates. Figure 1 illustrates the specific interactions used: we incorporate nearest-neighbor (NN) interactions  $\omega_1$  for CO pairs separated by distance  $a/\sqrt{2}$ , second NN (2NN) interactions  $\omega_2$  for separation  $a$ , third NN (3NN) interactions  $\omega_3$  for separation  $\sqrt{2}a$ , and sometimes fourth NN (4NN) interactions  $\omega_4$  for separation  $\sqrt{5}/2a$ . Also illustrated in the figure is the experimentally observed  $c(2\sqrt{2} \times \sqrt{2})R45^\circ$  ordered structure.

In applying our model to analyze the heat of adsorption and the adsorption isobars for CO/Pd(100), we need also information of the initial heat of adsorption at low coverage, which corresponds to the absorption energy of an

isolated CO molecule at a bridge site. This quantity was measured at 1.55 eV in an early experiment by Tracy and Palmberg,<sup>1</sup> and at 1.67 eV in more recent experiments.<sup>3,4</sup> Using density functional theory (DFT) incorporating the generalized gradient approximation (GGA), Eichler and Hafner<sup>5</sup> studied the potential energy surface for CO adsorption on Pd(100). They reported the adsorption energy for CO on a bridge site to 1.92 eV. This value is larger than the experimental estimate, but the trend that bridge sites are favored over top and hollow sites is consistent with experimental findings.

To analyze the above two-dimensional LG model, in this paper we use two standard yet powerful statistical mechanical techniques: the transfer matrix (TM) and the Monte Carlo (MC) methods. These two methods are often complementary. Using TM, one can always obtain the equilibrium free energy and other thermodynamic properties of the system. However, it is difficult to include long-range interactions using TM. For example, performing analysis on a system or strip of size  $M \times \infty$ , in order to include 3NN interaction  $\omega_3$ , it is necessary to consider all configurations of two columns spanning the strip. Thus, one must consider a total of  $2^{2M}$  configurations, if one does not reduce this number by exclusion and symmetry properties. On the other hand, it is relatively straight-forward to include long-range interactions using the MC method. However, standard MC can become inefficient, especially when there are strong repulsive ad-species interactions, or for low temperatures.

### III. $c(2\sqrt{2} \times \sqrt{2})R45^\circ$ ORDERING BELOW 0.5 ML

From the observation of  $c(2\sqrt{2} \times \sqrt{2})R45^\circ$  ordered structure, it has been deduced that lateral interactions between CO(ads) consist of strong NN and 2NN repulsions, and a weak 3NN repulsion. It has also been pointed out by Behm *et al.*<sup>3</sup> that the 3NN repulsion  $\omega_3$  should not be too strong, otherwise it would instead produce a  $(\sqrt{5/2} \times \sqrt{5/2})R18.4^\circ$  structure, which is not observed experimentally.

In order to quantify the effect of the 3NN interaction on the ordering of CO adsorbates, we conduct a study of the phase transitions of the lattice-gas model with very strong NN and 2NN repulsions (i.e., exclusion), and a finite 3NN repulsion ( $\omega_3 > 0$ ). Different aspects of this model has been studied previously, but the complete picture is not available.

In the case of no 3NN interactions ( $\omega_3 = 0$ ), it was found that there exists a very “weak” transition from a disordered phase to a semi-ordered phase upon increasing the CO coverage above about  $\theta_{\text{CO}} = 0.477$ .<sup>10</sup> At the maximum  $\theta_{\text{CO}} = 0.5$ , the semi-ordered phase consists of alternating half-filled diagonal rows of bridge sites which can slide with respect to each other without energy penalty. In the limit of very strong 3NN repulsion ( $\omega_3 = \infty$ ), it was found<sup>11</sup> that there is a first-order liquid-solid-like transition with increasing CO coverage. The

ordered phase has a  $(\sqrt{5/2} \times \sqrt{5/2})R18.4^\circ$  structure.

(Traditionally, results of the above studies are described with respect to the square lattice of bridge sites. This lattice is rotated by  $45^\circ$  from the square lattice of Pd(100) substrate atoms, and has twice the number of sites as Pd atoms. Thus, the coverage on this lattice satisfies  $\rho = 0.5\theta_{\text{CO}}$ . For  $\omega_3 = 0$ , the semi-ordered phase is commonly denoted as  $(2 \times 1)$  phase, although it has long-range order in one dimension only. It has a maximal coverage of  $\rho = 0.25$ . For  $\omega_3 = \infty$ , the ordered phase is described as  $(\sqrt{5} \times \sqrt{5})R26.6^\circ$  with respect to the square lattice of bridge sites.)

Our TM and MC study shows that as  $\omega_3$  increases from zero, the “weak” transition to the semi-ordered phase becomes stronger, and for larger 3NN repulsion, the transition converts to a first-order transition to the  $c(2\sqrt{2} \times \sqrt{2})R45^\circ$  ordered structure. This implies the existence of a tricritical point. From MC simulations, we estimate that this tricritical point is located at  $(\beta\mu^t, \beta\omega_3^t) = (5.2, 0.3)$ , where  $\beta = 1/(k_B T)$  and  $\mu$  denotes the chemical potential for the adsorbed CO (which is described in more detail in the following sections). The corresponding coverage is  $\theta_{\text{CO}} = 0.46$  (or  $\rho = 0.23$ ).

As  $\beta\omega_3$  further increases above approximately 1.9, there is another first-order transition, but this time, the transition is from the disordered phase to a  $(\sqrt{5/2} \times \sqrt{5/2})R18.4^\circ$  phase. Figure 2 shows our preliminary results directed towards mapping out the  $\mu$ - $\beta$  phase diagram of the model with NN and 2NN exclusion, and 3NN repulsion. It shows two first-order liquid-solid-like transitions (dashed lines) from disordered phase to either a  $c(2\sqrt{2} \times \sqrt{2})R45^\circ$  ordered phase, or a  $(\sqrt{5/2} \times \sqrt{5/2})R18.4^\circ$  ordered phase. Also there is a solid-solid-like transition from the  $(\sqrt{5/2} \times \sqrt{5/2})R18.4^\circ$  phase to the  $c(2\sqrt{2} \times \sqrt{2})R45^\circ$  phase. There is a tricritical point connecting the continuous and first-order transitions to the  $c(2\sqrt{2} \times \sqrt{2})R45^\circ$  phase. However, how the termination of the  $(\sqrt{5/2} \times \sqrt{5/2})R18.4^\circ$  transition line is not clearly determined from the existing analysis. It is likely that the transition line bends towards and merges with the  $c(2\sqrt{2} \times \sqrt{2})R45^\circ$  transition line sharply at around  $\beta\omega_3 = 1.9$ .

Under the framework of the lattice gas model with only repulsive interactions between neighboring pairs up to 3NN, one can conclude that  $\omega_3 < 0.5$  eV so that at room temperature, no  $(\sqrt{5/2} \times \sqrt{5/2})R18.4^\circ$  phase shall be observed. A caveat is that introducing further neighboring interactions can change the phase diagram significantly and the above constraint on the magnitude of  $\omega_3$  is no longer valid if longer-ranged interactions should be considered.

Based on the above analysis (and also our investigations in subsequent sections), we assign a value of  $\omega_3 = 0.03$  eV for the strength of the 3NN repulsive interactions. In the following analyses which include consideration of behavior for CO coverage above 0.5 ML, it is necessary to relax the constraint of 2NN exclusions.

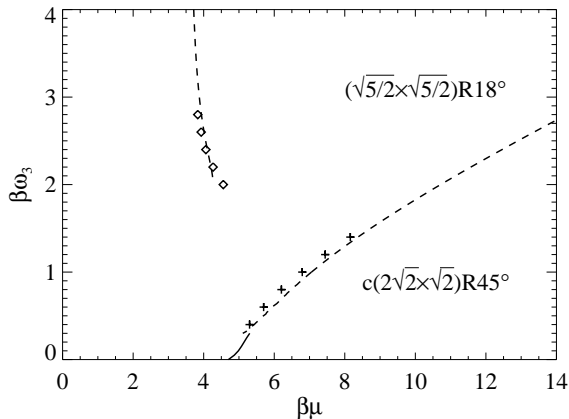


FIG. 2:  $\mu$ - $\theta$  phase diagram of the lattice-gas model with NN and 2NN exclusion and 3NN repulsion. The solid line denotes a continuous transition obtained from transfer matrix (TM) finite-size-scaling<sup>12</sup> (10-12 scaling). Also shown are two first-order transitions obtained from locating local maximum in  $d\theta/d\mu$  using two methods: the dashed lines are from TM (with strip of size 10) calculations, and the symbols are from Monte Carlo simulations with the histogram method.<sup>13</sup>

The value of  $\omega_2$  of around 0.17 eV is determined from our analysis of the heat of adsorption in Sec. V, and adsorption isobars in Sec. VI. However, before presenting these analyses, in Sec. IV, we provide a more complete picture of adlayer ordering by describing behavior at coverage above 0.5 ML (using the parameter choice  $\omega_1 = \infty$ ,  $\omega_2 = 0.17$  eV, and  $\omega_3 = 0.03$  eV.)

#### IV. STRUCTURE OF DENSE CO ADLAYERS

Because of the difficulties of experimental techniques (e.g., work function and infrared analysis) in dealing with high CO coverage ( $\theta_{\text{CO}} > 0.5$ ), structures of dense CO adlayers on Pd(100) are a matter of some debate.<sup>14,15,16</sup> As  $\theta_{\text{CO}}$  increases above 0.5 ML, it is concluded from diffraction studies that the adlayers structure undergoes a commensurate-incommensurate transition (CIT). The study by Schuster *et al.*<sup>16</sup> suggests it is in the Pokrovsky-Talapov universality class, consistent with expectation from symmetry arguments.

Lattice-gas models are not ideal for study of CIT's, since they put too many constraints on the structure of domain walls. Nonetheless, we perform a Monte Carlo study to investigate CO adlayer structure above 1/2 ML. We simulate the system at a fixed pressure while lowering the temperature. We use Glauber dynamics (corresponding to adsorption/desorption in the LG model) with the Metropolis algorithm. Occasionally, we also mix in Kawasaki dynamics (corresponding to diffusion in the LG model) with the Glauber dynamics. Here, our focus is in the equilibrium structure of CO adlayer, thus we do not need to mimic the physical kinetics accurately.

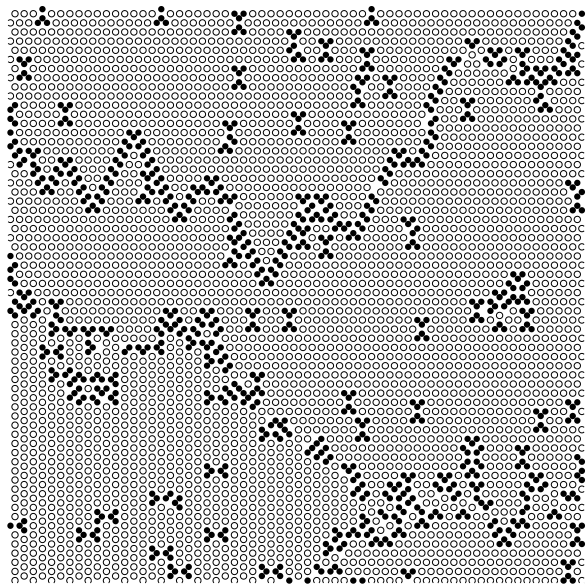


FIG. 3: Snapshot of Monte Carlo simulations using the Glauber dynamics and the Metropolis algorithm for the LG model at fixed pressure while lowering the temperature. The annealing rate is  $10^4$  MCS/K (each site in the system is sampled once on average for each MCS). Other parameters are  $p_{\text{CO}} = 10^{-7}$  Torr,  $\omega_1 = \infty$ ,  $\omega_2 = 0.17$  eV,  $\omega_3 = 0.03$  eV. The snapshot is taken at  $T = 400$  K. For illustration, we denote CO with exactly two 2NN and four 3NN by a circle, and all other CO (“defects”) by a black dot. Also note that the Pd(100) substrate (not shown) is rotated  $45^\circ$ . Shown in the figure is a  $L = 128$  subsystem in a simulation with  $L = 256$  using periodic boundary conditions.  $\theta_{\text{CO}} = 0.511$  ML.

The primary challenge is that due to CO adspecies repulsions, adlayers can become nearly “frozen” using normal dynamics at high CO coverage and low substrate temperature. In fact, the LG model with NN and 2NN exclusion has been used to study the glass transition.<sup>17</sup>

Although our simulations are not faithful to the physical adlayer dynamics, they provide at least some qualitative insights into adlayer structure. For a fixed system size with periodic boundary conditions, if we lower the temperature very slowly, eventually a single domain occupies the whole system. Upon further lowering the temperature, defects are formed. However, we are unable to observe any well-defined domain wall structure as suggested by Berndt and Bradshaw.<sup>15</sup> On the other hand, if we lower the temperature more quickly, then different domains still occupy the system near the transition point. Further decreasing the temperature is accompanied by the enlargement of those original domains, and emergence of defects inside different domains. We show in Fig. 3 a snapshot of such a configuration generated by Monte Carlo simulations.

## V. HEAT OF ADSORPTION

Assuming equilibrium between CO in the gas phase and the chemisorbed phase, the Clausius-Clapeyron equation relates the gas phase pressure,  $P$ , to an isosteric heat of adsorption,  $E_{st}$ , via

$$[d \ln P / d(1/T)]_{\theta} = -E_{st} / k_B. \quad (1)$$

Various experimental techniques<sup>1,3,18,19</sup> give similar results for the value of  $E_{st}$  as  $\theta_{CO} \rightarrow 0$ , while conflicting results have been obtained for the coverage dependence of  $E_{st}$ . Most studies<sup>1,18,19</sup> show a decrease in  $E_{st}$  with increasing  $\theta_{CO}$ , while the study by Behm *et al.*<sup>3</sup> shows a roughly constant  $E_{st}$  for  $\theta_{CO} < 0.5$ . Presence of carbon is suggested<sup>3</sup> as the reason for this discrepancy, a claim disputed by others.<sup>19</sup>

The presence of lateral interactions between CO adspecies is often invoked<sup>1,19</sup> to explain the coverage dependence of  $E_{st}$ . Yet to our knowledge, no systematic study of the isosteric heat of adsorption in an interacting lattice-gas model for this system has been performed previously. There are some general studies of effects of lateral interactions on the heat of adsorption using mean-field approximations (see, e.g., Ref. 20 and references therein) which are not reliable for models with relatively short-range interactions.

In lattice-gas modeling, it is appropriate to use the grand canonical ensemble. We assume simply that the gas phase pressure  $P$  is related to the chemical potential through  $\mu = k_B T \ln(P/P_0)$ . More accurate forms of the relationship between the pressure and the chemical potential will introduce corrections to the heat of adsorption on the order of  $k_B T$ , which is negligible for present purposes. Unlike the isobar experiments (treated later in Sec. VI), for our analysis here, we do not need information regarding prefactors for desorption, or the sticking coefficient for adsorption.

Using the transfer matrix method, we examine the coverage dependence of  $E_{st}$  for the lattice-gas model with various choices of interactions. Any coverage dependence would reflect the influence of adspecies interactions which can cause  $E_{st}$  to deviate from its limiting value of  $\epsilon_b$  for low coverage. Some of the results are shown in Fig. 4.

For the lattice gas model with only 2NN repulsive interaction only, the heat of adsorption is effectively a step function, with the form

$$E_{st} \approx \begin{cases} \epsilon_b & \text{if } \theta < 0.5 \\ \epsilon_b - 4\omega_2 & \text{if } 0.5 < \theta < 1. \end{cases} \quad (2)$$

The result can be explained as follows: for  $\theta < 0.5$ , adsorbed CO molecules can rearrange themselves to avoid any 2NN pairs. Around  $\theta = 0.5$ , they form a near-perfect  $c(2\sqrt{2} \times \sqrt{2})R45^\circ$  adlayer. To adsorb more CO molecules beyond this near-perfect overlayer, it is necessary to create four 2nd NN pairs. See Fig. 5 for an illustration.

With longer-ranged repulsive interactions,  $E_{st}$  decreases as  $\theta_{CO}$  increases even for  $\theta_{CO} < 0.5$ . However,

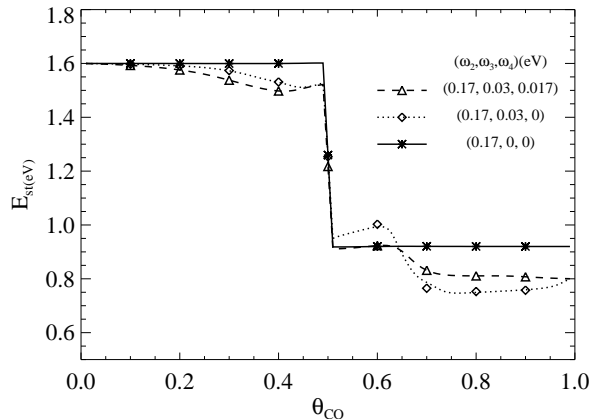


FIG. 4: Transfer matrix calculation of the isosteric heat of adsorption versus CO coverage on Pd(100). The lines are obtained using strips of size 8, and the symbols are obtained using strips of size 10. Nearest-neighbor interaction  $\omega_1$  is assumed to be infinite and other neighboring interactions are shown in the figure.  $T = 300$  K.

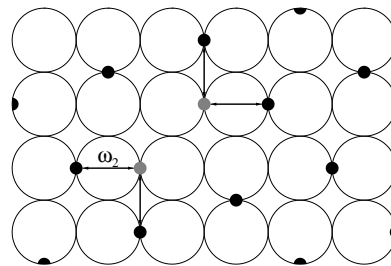


FIG. 5: Schematic showing the accommodation of an extra CO molecule in an otherwise perfect  $c(2\sqrt{2} \times \sqrt{2})R45^\circ$  structure.

the coverage dependence is quite nonlinear. For example, with 3NN interactions only (the dotted line),  $E_{st}$  only decreases slightly for  $\theta_{CO} < 0.25$ . This is again due to the fact that below this coverage, CO(ads) can easily arrange themselves in a way to avoid any 3NN pairs.

With the present set of parameters for lateral interactions, the lattice-gas model produces a coverage dependence of the heat of adsorption somewhat between the experimental results of Behm *et al.* and other groups. Most of the decrease in the heat of adsorption occurs when  $\theta_{CO} > 0.5$ , while only a slight decrease occurs when  $\theta_{CO} < 0.5$ .

The near parabolic decrease in  $E_{st}$  starting from  $\theta_{CO} = 0$ , as well as the transient increase after the ordering transition, shown by Fig. 4 are quite reminiscent to the experimental results of Guo and Yates<sup>21</sup> for CO adsorption on Pd(111). However, they reported a plateau at an ordering transition, while we see first a sharp drop and then a plateau at the ordering transition point.

FIG. 6: Adsorption isobars calculated from the lattice-gas model. Two sets of parameters are used.  $p_{\text{CO}}$  ranges from  $10^{-9}$  to 0.1 Torr.

## VI. ADSORPTION ISOBARS

For a CO adlayer in equilibrium with gas phase CO, it is clear that as the surface temperature increases (at fixed pressure), the CO coverage will decrease. For higher (fixed) pressures, this decrease will be delayed until a higher temperature range. To quantify this behavior using our LG model, one needs a more quantitative determination of the relationship between pressure and chemical potential than that presented in the previous section. To this end additional assumptions are needed. We assume that the impingement rate is given by  $P/\sqrt{2\pi mk_B T}$  and the attempt frequency for desorption is  $\nu_0$ , then we assume that

$$\mu = E_{\text{st}} + k_B T \ln \frac{P}{\nu_0 \sqrt{2\pi mk_B T}}. \quad (3)$$

The initial sticking coefficient when  $\theta_{\text{CO}} = 0$  is taken to be unity. Thus by assuming equilibrium of CO between gas phase and the chemisorption phase, one can calculate the adsorption isobar of the lattice gas model using either the transfer matrix or the Monte Carlo method.

The results are shown in Fig. 6. For low pressures, as  $T$  decreases,  $\theta_{\text{CO}}$  first increases, then reach a plateau at  $\theta_{\text{CO}} = 0.5$ . For  $p_{\text{CO}} = 10^{-7}$  Torr, the plateau occurs near  $T = 420$  K. This result is in very good agreement with experiments.<sup>3,18</sup> Upon a further decrease in temperature,  $\theta_{\text{CO}}$  again increases above 0.5 ML. Experimentally, this corresponds to the adlayer moving into the regime of the commensurate-incommensurate transition discussed in Sec. IV. Here, we simply note that the temperature where this occurs depends sensitively on the value of the 2NN interactions  $\omega_2$ . By choosing  $\omega_2 = 0.17$  eV, the transition occurs between 340 K to 400 K for  $p_{\text{CO}}$  between  $10^{-9}$  to  $10^{-7}$  Torr, in agreement with experiments.<sup>16,18</sup> It is also significant that at high pressures, the LG model predicts disappearance of the plateau near  $\theta_{\text{CO}} = 0.5$ , which is also observed experimentally.<sup>18</sup>

Note that we “naively” choose  $\nu_0 = 10^{13} \text{ s}^{-1}$  for the desorption prefactor, while Behm *et al.* obtain a value on the order of  $10^{16} \text{ s}^{-1}$  from their adsorption isobars. Consequently there is some discrepancy between the lattice-gas model prediction and experiments at low coverage. Specifically for  $\theta_{\text{CO}} < 0.5$  ML, significant desorption occurs at a higher temperature than experiments. Adopting adsorption energy  $\epsilon_b$  from DFT calculations and assuming the same prefactor makes the discrepancy even larger. Also the discrepancy will not likely be resolved by modification of interactions, since at low coverage lateral interactions are quite insignificant.

## VII. SUMMARY

We have performed a combined transfer matrix and Monte Carlo study of a lattice-gas model for CO adlayers on Pd(100). Model predictions are compared against a variety of experimental observations. Of particular significance is our determination of repulsive adspecies interactions:  $\omega_1 = \infty$ ,  $\omega_2 = 0.17$  eV, and  $\omega_3 = 0.03$  eV. Our estimate of the 2NN interaction of 0.17 eV agrees well with Wu and Metiu.<sup>6</sup> Our assignment of a weak 3NN interaction is consistent with early qualitative arguments by Behm *et al.*<sup>3</sup> Our use of a binding energy of  $\epsilon_b = 1.6$  eV in analysis of the heat of adsorption and the adsorption isobars is consistent with experimental estimates, but this value is somewhat smaller than that from DFT which is close to 2 eV.

## Acknowledgments

The author thank Profs. T. L. Einstein and P. A. Thiel for helpful discussions, and Prof. J. W. Evans for extensive discussion and suggestions. This work is supported by the Division of Chemical Sciences, U.S. Department of Energy (USDOE). It was performed at Ames Laboratory which is operated for the USDOE by Iowa State University under Contract No. W-7405-Eng-82.

<sup>1</sup> J. C. Tracy and P. W. Palmberg, *J. Chem. Phys.* **51**, 4852 (1969).

<sup>2</sup> A. M. Bradshaw and F. M. Hoffmann, *Surf. Sci.* **72**, 513 (1978).

<sup>3</sup> R. J. Behm, K. Christmann, G. Ertl, and M. A. Van Hove, *J. Chem. Phys.* **73**, 2984 (1980).

<sup>4</sup> J. Szanyi, W. K. Kuhn, and D. W. Goodman, *J. Vac. Sci. Techn. A* **11**, 1969 (1993).

<sup>5</sup> A. Eichler and J. Hafner, *Phys. Rev. B* **57**, 10110 (1998).

<sup>6</sup> M. W. Wu and H. Metiu, *J. Stat. Phys.* **113**, 1177 (2000).

<sup>7</sup> J. Wintterlin, S. Völkening, T. V. W. Janssens, T. Zam-

belli, and G. Ertl, *Science* **278**, 1931 (1997).

<sup>8</sup> D.-J. Liu and J. W. Evans (2003), in preparation.

<sup>9</sup> A. Ortega, F. M. Hoffmann, and A. M. Bradshaw, *Surf. Sci.* **119**, 79 (1982).

<sup>10</sup> F. H. Ree and D. A. Chestnut, *Phys. Rev. Lett.* **18**, 5 (1967).

<sup>11</sup> A. Bellemans and R. K. Nigam, *Phys. Rev. Lett.* **16**, 1038 (1966).

<sup>12</sup> M. P. Nightingale, *Physica* **83A**, 561 (1976).

<sup>13</sup> A. M. Ferrenberg and R. H. Swendsen, *Phys. Rev. Lett.* **61**, 2635 (1988).

- <sup>14</sup> P. Uvdal, P.-A. Karlsson, C. Nyberg, S. Andersson, and N. V. Richardson, *Surf. Sci.* **202**, 167 (1988).
- <sup>15</sup> W. Berndt and A. M. Bradshaw, *Surf. Sci. Lett.* **279**, L165 (1992).
- <sup>16</sup> R. Schuster, I. K. Robinson, K. Kuhnke, S. Ferrer, J. Alvarez, and K. Kern, *Phys. Rev. B* **54**, 17097 (1996).
- <sup>17</sup> S. S. Rao and S. M. Bhattacharjee, *Phys. Rev. A* **45**, 670 (1992).
- <sup>18</sup> J. Szanyi and D. Goodman, *J. Phys. Chem.* **98**, 2972 (1994).
- <sup>19</sup> Y. Y. Yeo, L. Vattuone, and D. A. King, *J. Chem. Phys.* **106**, 1990 (1997).
- <sup>20</sup> S. A. Al-Muhtaseb and J. A. Ritter, *J. Phys. Chem. B* **103**, 2467 (1999).
- <sup>21</sup> X. Guo and J. T. Yates, Jr., *J. Chem. Phys.* **90**, 6761 (1989).